Preparation and Physical Properties of Polycrystalline $(Bi_{1-x}Pb_x)_2Sr_2Ca_2Cu_3O_y$ High T_c Superconductors

M.S. Awan, M. Maqsood, S.A. Mirza, M. Yousaf, and A. Maqsood

$(Bi_{1-x}Pb_x)_2Sr_2Ca_2Cu_3O_y$ (x = 0.3) high critical transition temperature (T_c) superconductors are synthesized by the solid-state reaction method in polycrystalline form. X-ray diffraction (XRD) studies, direct current (dc) electrical resistivity measurements, scanning electron microscopic (SEM) studies, critical current density measurements, and zero-field alternating current (ac) susceptibility measurements are performed to investigate the physical changes, structural changes, and magnetic behavior of the superconducting samples. X-ray diffraction studies show that a high T_c phase exists with orthorhombic symmetry in the specimen. According to the XRD data, the lattice parameters of the high T_c phase were determined as a = 0.537(1) nm, b = 0.539(1) nm, and c = 3.70(1) nm. The compound exhibits a superconducting transition at 106 ± 1 K for zero resistance. The ac susceptibility measurements in zero field confirm the dc electrical resistivity results; hence both support the XRD results. The particle size and structural changes as a function of the cold-pressing and aging effect are also reported.

Keywords
superconductivity, dc electrical resistivity, ac magnetic susceptibility

1. Introduction

SINCE the discovery of superconductors of high T_c, a large worldwide flood of research in superconductivity has taken place (Ref 1). Recent studies on oxide superconductors revealed the existence of a superconducting phase exhibiting zero electrical resistivity at 107 K in the Bi-Pb-Sr-Ca-Cu-O system. Two phases exist (Ref 2): the low T_c phase (2212) and the high T_c phase (2223). Synthesis of the (2223) phase is more difficult than that of the (2212) phase. The addition of lead helps in the formation of the high T_c superconducting phase (Ref 3), but the exact mechanism of this process is not clear. According to some authors (Ref 4), a melt is made by the lead addition, which is favorable for the growth of the (2223) phase prior to (2212). On the other hand, some authors (Ref 5, 6) pointed out that the content of lead is greatly reduced by an increase in the time of synthesis. Many studies (Ref 7-9) showed that the concentration of lead in a superconducting system drops to zero with the passage of time. Therefore, additional research work is needed to specify the actual role of lead in the formation of the (2223) phase. Takano et al. (Ref 5) synthesized a Bi-Pb-Sr-Ca-Cu-O superconductor containing lead atoms for which they found the T_c (zero) at 107 K and a relatively large fraction of the high T_c phase. The present results agree well with Ref 5. The oxide superconductors in the $(Bi_{1-x}Pb_x)_2Sr_2Ca_2Cu_3O_y$ system were prepared with x = 0.3, and the T_c (zero) was found at 106 ± 1 K. This composition was used because use of x = 0.2 was undertaken in detail in Ref 9. Along with other physical properties, the aging effect is presented here. The ac zero-field magnetic susceptibility gives much more powerful data for characterizing the superconducting specimen and discriminating between intergrain and intragrain properties (Ref 10). This study also aimed to find the proper conditions in terms of temperature and composition for preparation of single crystals as reported in Ref 11.

M.S. Awan, M. Maqsood, S.A. Mirza, M. Yousaf, and **A. Maqsood,** Thermal Physics Laboratory, Department of Physics, Quaid-i-Azam University, Islamabad, Pakistan 45320

2. Experimental

Samples were prepared from powders of Bi_2O_3, PbO, $SrCO_3$, $CaCO_3$, and CuO. All the materials were 99.9% pure. Powders were mixed to give the starting nominal composition of $(Bi_{1-x}Pb_x)_2Sr_2Ca_2Cu_3O_y$. The mixture was calcined at 800 ± 5 °C and grinded in the repeating steps for 2 h. After the pellet formation, the samples were sintered at 845 ± 5 °C for 24 h. Three samples, 1, 2, and 3, were prepared under different pressures of 178, 355 MPa (2 and 4 tons/cm^2) and hand pressure, respectively. These samples were sintered for 516, 630, and 576 h accordingly. Resistivity as a function of temperature was measured by a standard dc four-probe method with an exciting current of 10 mA. Figure 1 shows the influence of annealing time on the resistivity as a function of temperature for sample 2.

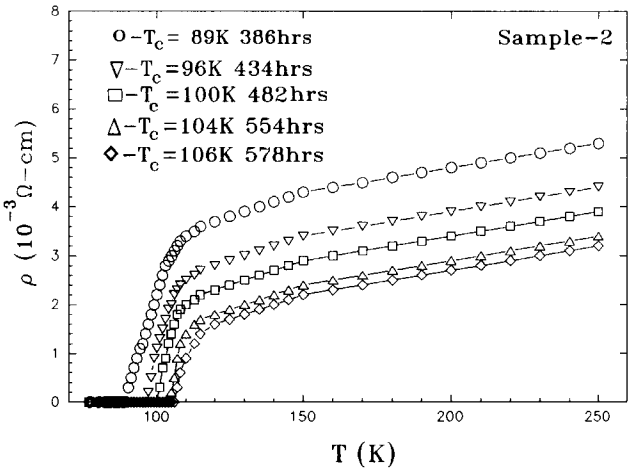

Fig. 1 The T_c (zero) as a function of annealing time from resistivity measurements of sample 2 for the $Bi_{1.4}Pb_{0.6}Sr_2Ca_2Cu_3O_y$ compound

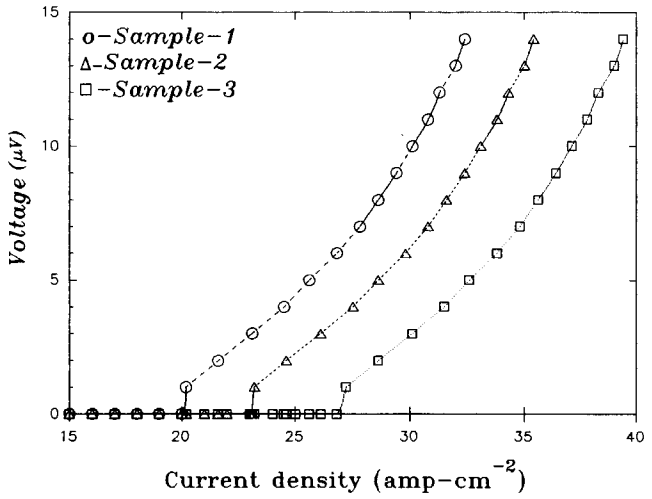

Fig. 2 Current density vs. voltage in zero field at 77 K for $Bi_{1.4}Pb_{0.6}Sr_2Ca_2Cu_3O_y$

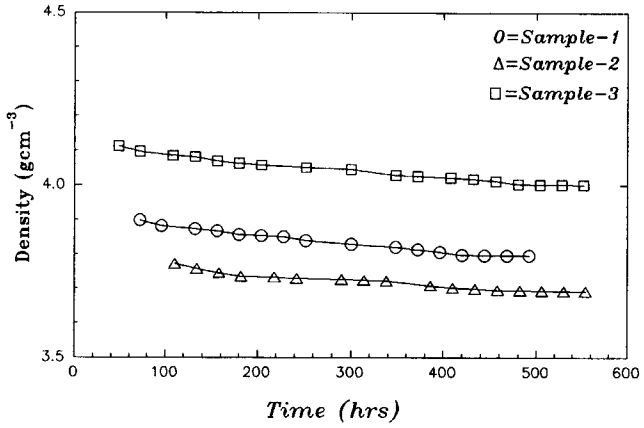

Fig. 3 Apparent density of the samples vs. annealing time

Critical current density of the samples was measured at 77 K in zero magnetic field as shown in a graph of current density vs. voltage in Fig. 2. Again suggesting the importance of pressing pressure, Fig. 3 shows the annealing time dependence of the apparent density of three samples. For XRD information, the Debye-Scherrer powder method was adopted in order to determine the lattice parameters of the unit cell. For this purpose, CuK_α (0.15418 nm) radiation was used with tube current and voltage of 30 mA and 40 kV, respectively. The exposure time was 4 h. Samples were mounted in a glass capillary having a diameter of 0.2 mm and a wall thickness of 0.01 mm. The measured lattice parameters for the high T_c phase were a = 0.537(1) nm, b = 0.539(1) nm, and c = 3.70(1) nm. Few peaks of the low T_c phase were also detected. Information about grain size, crystal shape, and bulk density of the samples was collected by the SEM studies. For zero-field ac susceptibility measurements, the low ac field (0.5 Oe) is applied parallel to the axis of the rectangular, rod-shaped specimen, which is in the central part surrounded by a pick-up coil. From the output

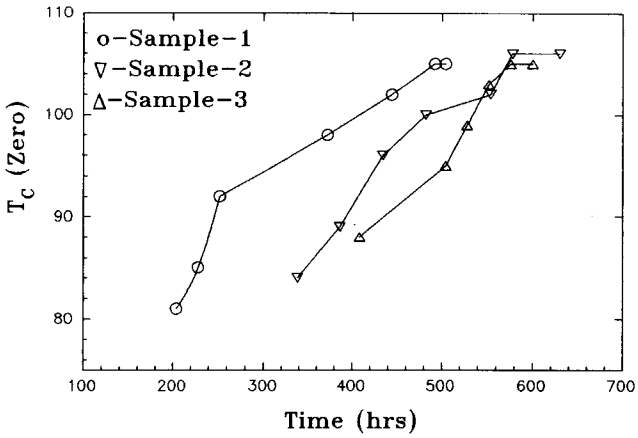

Fig. 4 Annealing time vs. the T_c (zero) for $Bi_{1.4}Pb_{0.6}Sr_2Ca_2Cu_3O_y$

signal of the pick-up coil, the superconducting behavior of the sample is observed. The in-phase and out-of-phase components of this signal are detected by a lock-in amplifier corresponding to the real, χ', and imaginary, χ'', parts of the ac susceptibility. The real or in-phase part, χ', of complex ac susceptibility χ shows the diamagnetic transition as a function of temperature seeking information about the transition temperature, different phases (if any), the granularity, and sensitivity to the applied magnetic field. Imaginary or out-of-phase part, χ'', shows ac losses and the nature of intergrain weak links in the materials.

3. Results and Discussion

Three samples with starting composition $(Bi_{1-x}Pb_x)_2Sr_2Ca_2Cu_3O_y$ (x = 0.3) were prepared under different pressures of 178, 355 MPa (2 and 4 tons/cm^2), and hand pressure, and named sample 1, 2, and 3, respectively. Their detailed information about dc electrical resistivity measurements, aging effect, critical current measurements, annealing time dependence of apparent density, XRD studies, ac susceptibility measurements, and SEM studies are given below.

3.1 *Resistivity and Critical Current Measurements*

Direct current electrical resistivity measurements reveal that pressing pressure did not show any remarkable effect upon the T_c of the samples. A standard dc four-probe method showed that maximum T_c for zero resistance was 106 ± 1 K for sample 2, which was annealed for 630 h as shown in Fig. 1. The T_c (zero) and annealing time for three samples is shown in Fig. 4. The T_c for zero resistance increases with increase of annealing time. After a critical annealing time, the T_c (zero) remains the same for all the samples. This result shows that the intended composition was in the high T_c phase. Pressure showed tremendous effect for the critical current density measurements. Increase of pressure increases the critical current through the specimen. This increment may be due to the fact that the increase of pressure increases the area of contact between the grains and particles. Maximum critical current density is 27.20

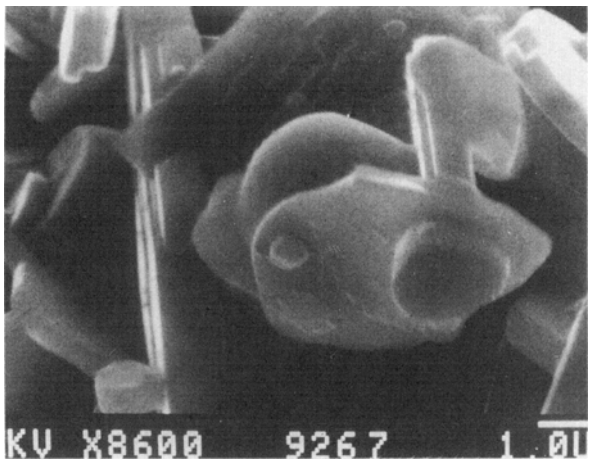

(a)

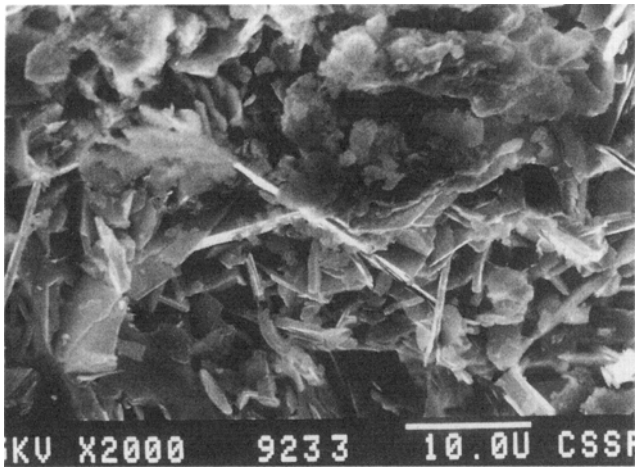

(b)

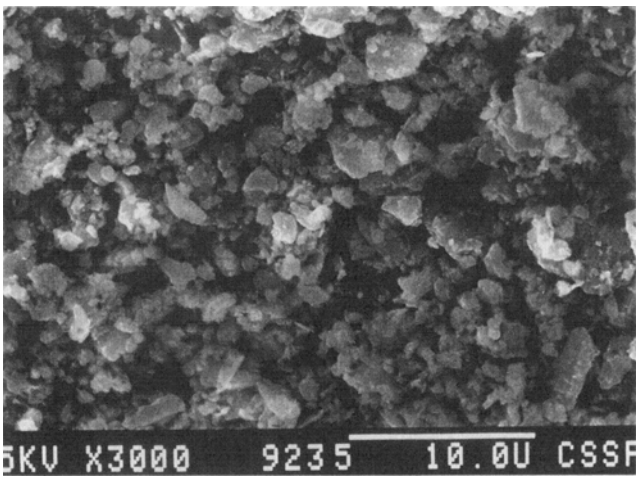

(c)

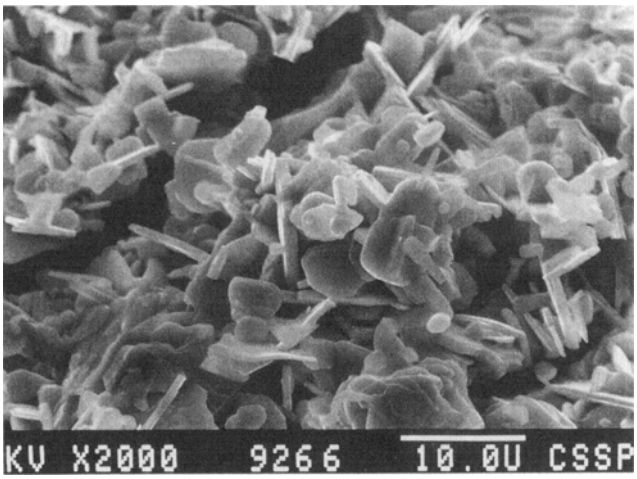

(d)

Fig. 5 Scanning electron micrographs from the specimen pressed under (a) hand pressure, (b) 2 ton/cm^2 pressure, and (c) 4 ton/cm^2 pressure. (a) Shows platelike crystal growth. (b) Shows grains having sharp boundaries. (c) Shows small, round-shaped crystals. (d) Sample 1 shows a crack through the bulk of the specimen.

A/cm^2 for sample 3, which was pressed with a pressure of 355 MPa (4 ton/cm^2). The apparent density of the samples decreases with the increase of annealing time as shown in Fig. 3. The average decrease in density after 630 h sintering for the three samples was 2.5%. Decrease was rapid for the first few sinterings, but after 450 h sintering, density of the samples remains virtually constant.

3.2 *X-Ray Diffraction Studies*

For XRD information, the Debye-Scherrer powder method was adopted. Along with the high T_c phase, a few peaks of the low T_c phase were also observed. Lattice parameters of the high T_c phase are $a = 0.537(1)$ nm, $b = 0.539(1)$ nm, and $c = 3.70(1)$ nm. Lattice parameters of the high T_c phase are identical to the (2223) phase, and those of the low T_c phase correspond to the (2212) phase. The high T_c phase in the Bi-Pb-Sr-Ca-Cu-O system is due to the substitution of lead atoms by bismuth atoms (Ref 3). This phase is unstable and decomposes into the low T_c phase with the increase of time of synthesis (Ref 5-6).

3.3 *Scanning Electron Microscopic Studies*

Scanning electron microscopic studies showed that the pressing pressure applied for green pellet compacts produces a remarkable effect upon the grain size, crystal shape, and bulk density of the samples. Samples 1 and 2 showed platelike crystal growth as shown in Fig. 5(a) and (b). The average grain size of the crystals was 7 to 8 μm and 4 to 5 μm for the two samples, respectively. The grains of sample 1 usually had flake-like structure, and secondary crystallization was also observed as shown in Fig. 5(a). The pores were large and occurred in the

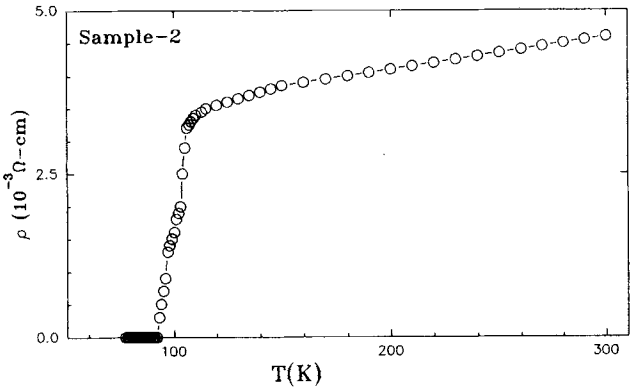

Fig. 6 Temperature dependence of resistivity of $Bi_{1.4}Pb_{0.6}Sr_2Ca_2Cu_3O_y$ sample 2 studied after two years of preparation

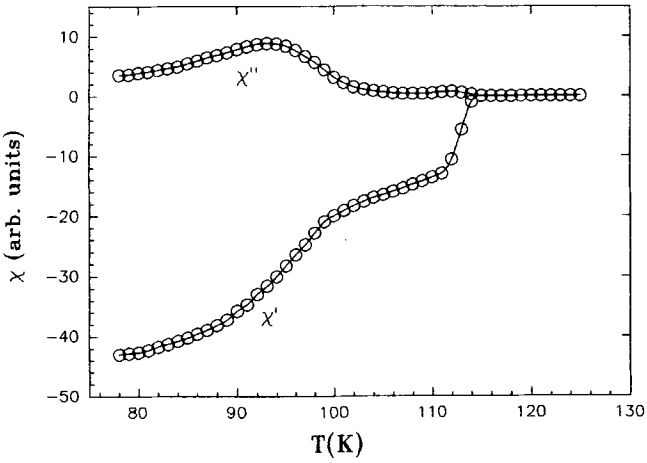

Fig. 7 Real and imaginary part of susceptibility vs. temperature for sample 2 of the $Bi_{1.4}Pb_{0.6}Sr_2Ca_2Cu_3O_y$ compound at 0.5 Oe and 240 Hz

form of long channels, which provided room for grain growth. Average grains in sample 2 possessed sharp boundaries and were occasionally mixed with flat-shaped crystals. Because of high pressure, flake-like crystals, large pores, and sharp boundaries were reduced to small, round-shaped crystals for sample 3. Figure 5(c) shows very little platelike crystal. Pores typically had dimensions of approximately $1.5 \times 1.0\ \mu m^2$ and were evenly distributed throughout the material. The pore density was lower in the sample prepared under high pressure, which increases the contact area between the particles. This increase is responsible for the higher value of current density for sample 3. Cracks were also observed on the surface of the specimen. There is a crack of about 3 to 4 μm through the bulk of the sample as shown in Fig. 5(d). This may be due to the thermal shocks or uncontrolled cooling rates when power was suddenly cut off.

3.4 *Aging Effect*

In order to investigate the aging effect in the Bi-based high T_c superconductors, dc electrical resistivity and zero-field ac susceptibility measurements were repeated on sample 2 after two years of preparation. As discussed above, the sample was almost the high T_c phase, and the low T_c phase could not be detected by the dc electrical resistivity vs. temperature curve as shown in Fig. 1, although XRD data showed the presence of a few peaks of the low T_c phase. As is obvious from Fig. 6, the low T_c phase appeared in the dc electrical resistivity vs. temperature curve. Therefore, the high T_c Phase decomposes into the low T_c phase after two years. Perhaps this happens because the concentration of lead, which is responsible for the formation of the high T_c phase, decreases with the passage of time and decomposes into the low T_c phase. Pb sits in the place of Bi because the ionic size of Pb and Bi are similar. For resistivity measurement, two phases were observed. Onset of the first phase lies at 114 ± 1 K. The second-phase transition starts at 99 ± 1 K, and finally, resistance drops to zero at 92 ± 1 K. These results, shown in Fig. 6, agree well with the zero-field ac susceptibility as described below.

3.5 *Susceptibility Measurements*

Sample 2 was taken for zero-field ac susceptibility measurements after two years of preparation. The experiment was carried out by applying an ac field of 0.5 Oe and frequency of 240 Hz. Remaining in the Meissner region and observing the diamagnetic transitions with more precision is ensured by low-field measurement. Measurement of the real part, χ', of the ac susceptibility on this sample clearly shows that there are two phases present; see Fig. 7. Onset of the first phase is at 114 ± 1 K. This phase shows a very sharp drop, which ends at 112 ± 1 K giving a transition width of 2 K. The second phase starts at 100 ± 1 K and has comparatively slow transition giving a broad transition width. The real part of ac susceptibility vs. temperature is shown in Fig. 7. The imaginary part of susceptibility, χ'', has a well-defined peak at temperature 92 ± 1 K with onset around 100 K. This peak has approximately the same transition width as observed in the second-phase transition of the real part. A small peak also appears at 112 ± 1 K, starting from 114 ± 1 K and varying very sharply within 2 K. Both peaks in the imaginary part are showing energy losses taking place in the intragrain and the intergrain regions, respectively, during transition from the normal to the superconducting state. The overall broad transition width of the two phases clearly defines the polycrystalline structure of the specimen. Information about the real and the imaginary part of susceptibility vs. temperature is shown in Fig. 7. These results agree well with results of the Bi-based granular samples reported in Ref 12.

4. Conclusions

It is possible to synthesize the $(Bi_{1-x}Pb_x)_2Sr_2Ca_2Cu_3O_y$ (with $x = 0.3$) compound by a solid-state reaction with the almost pure high T_c phase with T_c (zero) ≈106 ± 1 K. The detail studies of this compound by XRD, dc electrical resistivity, current density measurements, ac susceptibility in zero field, and SEM studies are reported. The aging effect is observed in this compound when one of the samples was reexamined by dc

electrical resistivity and ac susceptibility measurements after two years of preparation. Both measurements show that two phases exist: (2223) and (2212). Part of the high T_c phase (2223) converts into the low T_c phase (2212). Therefore, the high T_c phase is unstable and decomposes into a low T_c phase with the passage of time. From resistivity measurements, the T_c (onset) of the first phase is 114 ± 1 K, and the T_c (zero) for the second phase is 92 ± 1 K. On the other hand, from susceptibility measurements, the onset of the first-phase transition in the real part is 114 ± 1 K, and that of the second phase is 100 ± 1 K.

Acknowledgments

Many thanks to Dr. S.A. Siddiqui of Centre for Solid State Physics, Lahore, for providing the electron micrographs. Muhammad Arshad, Shahid Mahmood Ramay, and Miss Zahida Ali are thanked for useful discussion on the experiments.

References

1. J.G. Bednorz and K.A. Muller, *Z. Phys. B*, Vol 64, 1986, p 189
2. N. Shun-Ichi, O. Hiroshi, I. Ienari, and Y. Ryozo, *Jpn. J. Appl. Phys.*, Vol 28, 1989, p L27
3. S.A. Sunshine, *Phys. Rev. B*, Vol 38, 1988, p 893
4. T. Hatano, K. Aota, S. Idea, K. Nakamura, and K. Ogawa, *Jpn. J. Appl. Phys.*, Vol 27, p L2055
5. M. Takano, J. Takada, K. Oda, H. Kitaguchi, Y. Miura, Y. Ikeda, Y. Tomii, and H. Mazaki, *Jpn. J. Appl. Phys.*, Vol 27, 1988, p L1041
6. K. Togano, H. Kumakura, H. Meada, E. Yanagisawa, and K. Takahasi, *Appl. Phys. Lett.*, Vol 53, 1988, p 1329
7. S.K. Dew, N.R. Osborne, P.J. Mulhem, and R.R. Parsons, *Appl. Phys. Lett.*, Vol 54, 1989, p 1929
8. A. Maqsood, N.M. Bhatti, S. Ali, and I. Haq, *J. Mater Res. Bull.*, Vol 25, 1990, p 779
9. A. Maqsood, S. Ali, M. Maqsood, I. Haq, and M. Khaliq, *J. Mater Sci.*, Vol 27, 1992, p 2363
10. H. Kuper, I. Apfelstedt, R. Flukiger, C. Keller, R. Meier-Hirmer, B. Runtsch, A. Turowski, U. Wiech, and T. Wolf, *Cryogenics*, Vol 28, 1988, p 650
11. M.S. Awan, M. Maqsood, G. Shabbir, A. Maqsood, S.A. Mirza, and S.A. Siddiqui, *J. Mater Sci. Lett.*, Vol 13, 1994, p 741
12. A. Ono, *Jpn. J. Appl. Phys.*, Vol 27, 1988, p L2276